



# Threshold Voltage Model for Symmetric Double-Gate (DG) MOSFETs With Non-Uniform Doping Profile

PRAMOD KUMAR TIWARI\* and S.JIT

Centre for Research in Microelectronics (CRME), Department of Electronics Engineering,  
Institute of Technology, Banaras Hindu University,  
Varanasi-221005

INDIA

\*[pramod.tiwari.ece09@itbhu.ac.in](mailto:pramod.tiwari.ece09@itbhu.ac.in)

**Abstract:** - The paper presents a two-dimensional (2D) model for the potential distribution and threshold voltage of symmetric double-gate MOSFETs (DG MOSFETs) with a Gaussian doping profile in the vertical direction of the channel. The 2D Poisson's equation is solved with suitable boundary conditions in the channel region to obtain the channel potential of the device. The expression for the threshold voltage is obtained by calculating the total charge crossing the virtual cathode and setting its value equal to the peak channel doping. The threshold voltage dependence on the channel length, channel doping, silicon channel thickness and gate oxide thickness are also discussed. The results are well matched with the simulation results obtained by using the commercially available 2D ATLAS™ device simulator.

**Key-Words:** - Poisson's equation, 2D channel potential, threshold voltage, threshold roll-off, Gaussian doping, ATLAS

## 1 Introduction

Bulk MOSFETs show the severe short channel effects like drain induced barrier lowering (DIBL) and threshold voltage roll-off as the channel length of device goes down in sub-50 nm range. The controllability of the gate voltage on the channel charge degrades severely as a result. Double-Gate (DG) MOSFETs are the good candidate to replace the conventional MOSFETs in this particular region because of their excellent immunity to the short channel effects [1-8]. The roles of threshold voltage become increasing important with IC applications targeting low-voltage, low-power and high speed applications. Various attempts have been made to

model the threshold voltage of DG MOSFETs [9-13]. Bhattacharjee et al. [9] presented a threshold voltage model by considering the minimum channel potential equal to the twice of Fermi voltage. The short channel threshold voltage models of DG MOSFETs presented by Tsormpatzoglou et al. [10] and Hamid et al. [11] considered the threshold voltage as a gate voltage at which the minimum carrier charge sheet density  $Q_{inv}$  reaches a value  $Q_{TH}$  adequate to achieve the device turn-on condition. The threshold voltage model reported by Kang et al. [12] included the effect of localized charges in the device. Kranti et al. [13] included the effect of lateral source drain doping gradient and the spacer width on the threshold voltage. However, all the models discussed above for DG MOSFETs are based on the assumptions of a uniformly doped channel of the device. Recently, Zhang et al. [14] has reported a 2D model for the potential distribution and threshold voltage of fully depleted SOI MOSFETs with a vertical Gaussian profile in the channel. It may be mentioned that the practical MOSFETs have a Gaussian distributed doping profile in the channel due to the requirement of many implantation and diffusion steps during fabrication process, such as threshold adjust implantation. Thus, modeling of 2D potential distribution and threshold voltage with a Gaussian doping profile may provide some better physical characteristics of real DG MOSFETs.

This paper presents a 2D model for potential distribution and threshold voltage with a Gaussian distributed channel doping profile along the vertical direction of the channel with profile parameters  $R_p$  and  $\sigma_p$  as projected range and straggle respectively.

For the symmetry of the device structure, the peak of the profile is assumed to be located at the middle of the channel thickness. The model solves the 2D

Poisson's equation with suitable boundary conditions to obtain the potential distribution function in the channel. The threshold voltage expression is obtained as the gate voltage at which the sum of electron density at the back and front surface equals the peak doping density of the silicon channel as considered in [15]. The effects of channel length, silicon film thickness and the gate oxide thickness on the threshold voltage are also discussed. Our model results are found to be well matched with the simulation results obtained by the commercially available ATLAS<sup>TM</sup> [16] 2D device simulator.

## 2 Theoretical model

The schematic structure of a DG MOSFET used for our analysis and simulation is shown in Fig.1 where  $L, t_{si}$  and  $t_{ox}$  are the gate-length, channel thickness and gate-oxide thickness of the device respectively. The x- and y- axes of the 2D structure are considered to be along the source-channel interface and channel-upper oxide interface as shown in the figure.

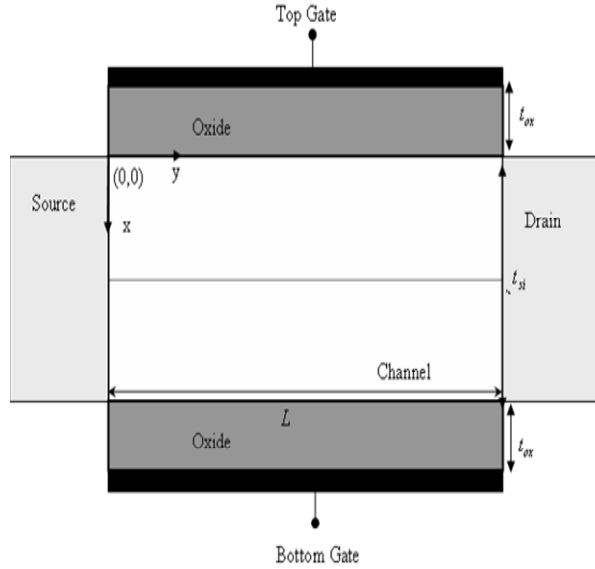


Fig.1: Schematic structure of symmetric DG MOSFET.

Let  $N_b(x)$  be the vertical doping profile in the p-type SOI film. We can express  $N_b(x)$  as [14]

$$N_b(x) = N_p \exp\left(-\left(\frac{x - R_p}{\sqrt{2}\sigma_p}\right)^2\right) \quad (1)$$

where,  $N_p$  is the doping concentration at the projected range  $R_p$  with a straggle  $\sigma_p$ .

Let  $\psi(x, y)$  be the 2D potential distribution function in the channel. Now,  $\psi(x, y)$  can be obtained by solving 2D Poisson's equation

$$\frac{\partial^2 \psi(x, y)}{\partial x^2} + \frac{\partial^2 \psi(x, y)}{\partial y^2} = \frac{qN_b(x)}{\epsilon_{si}} \quad (2)$$

with the following boundary conditions [9]

$$\psi(x, y)|_{x=0} = \psi_s(y) \quad (3)$$

$$\frac{\epsilon_{ox}}{t_{ox}} [V_G - V_{fb} - \psi(0, y)] = -\epsilon_{si} \frac{\partial \psi}{\partial x} \Big|_{x=0} \quad (4)$$

$$\frac{\epsilon_{ox}}{t_{ox}} [V_G - V_{fb} - \psi(t_{si}, y)] = \epsilon_{si} \frac{\partial \psi}{\partial x} \Big|_{x=t_{si}} \quad (5)$$

$$\psi(x, 0) = V_{bi} \quad (6)$$

$$\psi(x, L) = V_{bi} + V_{DS} \quad (7)$$

where  $\psi_s$  is the channel surface potential,  $\epsilon_{si}$  is the permittivity of silicon,  $\epsilon_{ox}$  is the permittivity of the gate-oxide  $\text{SiO}_2$ ,  $V_{bi}$  is the built-in potential,  $V_{fb}$  is the flat-band voltage,  $V_G$  is the gate-source voltage and  $V_{DS}$  is the drain-source voltage.

By introducing a variable  $\tau$  as  $\tau = \frac{x - R_p}{\sqrt{2}\sigma_p}$ , Eqs. (2)

and boundary conditions described by Eqs.(3)-(7) can respectively be modified as

$$\frac{1}{2\sigma_p^2} \frac{\partial^2 \psi(\tau, y)}{\partial \tau^2} + \frac{\partial^2 \psi(\tau, y)}{\partial y^2} = \frac{qN_p}{\epsilon_{si}} \exp(-\tau^2) \quad (8)$$

$$\psi(\tau, y)|_{\tau=B} = \psi_s(y) \quad (9)$$

$$\frac{\epsilon_{ox}}{t_{ox}} [V_G - V_{fb} - \psi(B, y)] = -\frac{\epsilon_{si}}{\sqrt{2}\sigma_p} \frac{\partial \psi}{\partial \tau} \Big|_{\tau=B} \quad (10)$$

$$\frac{\epsilon_{ox}}{t_{ox}} [V_G - V_{fb} - \psi(A, y)] = \frac{\epsilon_{si}}{\sqrt{2\sigma_p}} \frac{\partial \psi}{\partial \tau} \Big|_{\tau=A} \quad (11)$$

$$\psi(\tau, 0) = V_{bi} \quad (12)$$

$$\psi(\tau, L) = V_{bi} + V_{DS} \quad (13)$$

$$\text{where, } A = \frac{t_{si} - R_p}{\sqrt{2\sigma_p}} \text{ and } B = \frac{-R_p}{\sqrt{2\sigma_p}} \quad (14)$$

Using the method proposed by Zhang et al [14], the modified 2D Poisson's equation described by Eq. (8) can be solved to express the 2D channel potential function  $\psi(\tau, y)$  as

$$\psi(\tau, y) = C_0(y) + C_1(y)\tau + C_2(y) \times \left[ \tau \operatorname{erf}(\tau) + \frac{\exp(-\tau^2)}{\sqrt{\pi}} \right] \quad (15)$$

where  $C_0(y)$ ,  $C_1(y)$  and  $C_2(y)$  are arbitrary functions of  $y$  to be determined by using the modified boundary conditions described by Eqs.(9)-(11) and

$$\operatorname{erf}(\tau) = \frac{2}{\sqrt{\pi}} \int_0^\tau \exp(-t^2) dt \quad (16)$$

is called the error function.

Applying the boundary conditions described by Eqs. (9) to (11) in Eq. (15) we obtain

$$C_0(y) = V_G - V_{fb} + KC_2(y) \quad (17)$$

$$C_1(y) = -PC_2(y) \quad (18)$$

$$C_2(y) = \frac{(\psi_s - V_G + V_{fb})}{\left( K - PB + \operatorname{Berf}(B) + \frac{\exp(-B^2)}{\sqrt{\pi}} \right)} \quad (19)$$

where,

$$P = \left\{ t_{ox} \frac{\epsilon_{si}}{\epsilon_{ox} \sqrt{2\sigma_p}} \operatorname{erf}(B) - \operatorname{Berf}(B) - \frac{\exp(-B^2)}{\sqrt{\pi}} \right.$$

$$\left. + A \operatorname{erf}(A) + \frac{\exp(-A^2)}{\sqrt{\pi}} + t_{ox} \frac{\epsilon_{si}}{\epsilon_{ox} \sqrt{2\sigma_p}} \operatorname{erf}(A) \right\} \times \left( 2t_{ox} \frac{\epsilon_{si}}{\epsilon_{ox} \sqrt{2\sigma_p}} - B + A \right)^{-1} \quad (20)$$

$$K = P \left( A + t_{ox} \frac{\epsilon_{si}}{\epsilon_{ox} \sqrt{2\sigma_p}} \right) - A \operatorname{erf}(A) - \frac{\exp(-A^2)}{\sqrt{\pi}} - t_{ox} \frac{\epsilon_{si}}{\epsilon_{ox} \sqrt{2\sigma_p}} \operatorname{erf}(A) \quad (21)$$

To find the surface potential  $\psi_s$ , solving the Poisson equation described by Eq. (8) at the upper Si-SiO<sub>2</sub> interface gives

$$\frac{1}{2\sigma_p^2} \frac{\partial^2 \psi(\tau, y)}{\partial \tau^2} \Big|_{\tau=B} + \frac{\partial^2 \psi(\tau, y)}{\partial y^2} \Big|_{\tau=B} = \frac{qN_p}{\epsilon_{si}} \exp(-\tau^2) \Big|_{\tau=B} \quad (22)$$

With the help of Eqs.(15) (17) and(18), Eq.(22) can be modified as

$$\frac{\partial^2 \psi_s}{\partial y^2} + \frac{V_G - V_{fb} - \psi_s}{\lambda^2} = \frac{qN_p}{\epsilon_{si}} \exp(-B^2) \quad (23)$$

where,

$$\lambda = \sqrt{\pi} \sigma_p^2 \left( \frac{PB - K - \operatorname{Berf}(B) - \frac{\exp(-B^2)}{\sqrt{\pi}}}{\exp(-B^2)} \right) \quad (24)$$

is called the characteristic length associated with the surface potential  $\psi_s$ .

Equation (23) can be solved to obtain the surface potential as

$$\psi_s = k_1 \exp\left(\frac{y}{\lambda}\right) + k_2 \exp\left(-\frac{y}{\lambda}\right) + V_G - V_{fb} - \lambda^2 \frac{qN_p}{2\epsilon_{si}} \exp(-B^2) \quad (25)$$

where  $k_1$  and  $k_2$  are arbitrary constants. Using the boundary conditions described by Eqs. (12) and (13) in Eq.(25),  $k_1$  and  $k_2$  can be expressed as

$$k_1 = D - QV_G \quad (26)$$

$$k_2 = E - RV_G \quad (27)$$

where  $\alpha = \frac{L}{\lambda}$ ; and

$$D = \left( \frac{V'_{bi}(\exp(-\alpha) - 1) - V_{DS}}{\exp(-\alpha) - \exp(\alpha)} \right) \quad (28)$$

$$E = \left( \frac{V'_{bi}(\exp(\alpha) - 1) - V_{DS}}{\exp(\alpha) - \exp(-\alpha)} \right) \quad (29)$$

$$Q = \left( \frac{\exp(-\alpha) - 1}{\exp(-\alpha) - \exp(\alpha)} \right) \quad (30)$$

$$R = \left( \frac{\exp(\alpha) - 1}{\exp(\alpha) - \exp(-\alpha)} \right) \quad (31)$$

$$V'_{bi} = \left( V_{bi} + V_{fb} + \lambda^2 \frac{qN_p}{\epsilon_{si}} \exp(-B^2) \right) \quad (32)$$

From Eqs.(15), (17), (18),(19) the 2D channel potential  $\psi(\tau, y)$  can be expressed as

$$\psi(\tau, y) = V_G - V_{fb} + \left( K - P\tau + \tau \operatorname{erf}(\tau) + \frac{\exp(-\tau^2)}{\sqrt{\pi}} \right) \times \left( \frac{(\psi_s - V_G + V_{fb})}{K - PB + \operatorname{Berf}(B) + \frac{\exp(-B^2)}{\sqrt{\pi}}} \right) \quad (33)$$

Now, suppose that  $\psi_s = \psi_{s \min} = \psi_s(y_{s \min})$  represents the minimum value of  $\psi_s(y)$  at  $y = y_{s \min}$  where the distance  $y_{s \min}$  can be obtained by solving  $\left. \frac{d\psi_s(y)}{dy} \right|_{y=y_{s \min}} = 0$

which gives

$$y_{s \min} = \sqrt{\frac{\lambda}{8}} \ln\left(\frac{k_2}{k_1}\right) \quad (34)$$

From Eqs. (25) and (34), we can thus obtain

$$\psi_{s \min} = 2\sqrt{k_1 k_2} + V_G - V_{fb} - \lambda^2 \frac{qN_p}{2\epsilon_{si}} \exp(-B^2) \quad (35)$$

Following the method described in Ref. [15], the threshold voltage of short channel DG MOSFETs can be defined as the gate voltage where sum of the electron densities at the back and front surfaces after inversion reaches the peak acceptor doping density. Applying the above definition, the minimum surface potential can be found as

$$\frac{2n_i^2}{N_p \exp(-B^2)} \exp\left(\frac{q\psi_{s \min-th}}{kT}\right) = N_p \quad (36)$$

and hence

$$\psi_{s \min-th} = 2V_T \ln\left(\frac{N_p}{n_i} \sqrt{\frac{\exp(-B^2)}{2}}\right) \quad (37)$$

where  $V_T$  and  $n_i$  are the thermal potential and the intrinsic concentration of the silicon channel film. Substituting  $\psi_{s \min}$  by  $\psi_{s \min-th}$ ,  $V_G = V_{th}$  and using Eqs. (26)-(27) in Eq.(35), we can write

$$V_{th} = \left[ \psi_{s \min-th} + V_{fb} + \frac{\lambda^2 qN_p}{2\epsilon_{si}} \exp(-B^2) \right] - 2\sqrt{(D - QV_{th})(E - RV_{th})} \quad (38)$$

where  $V_{th}$  is assumed to be the threshold voltage of the short-channel DG MOSFET device.

It may be noted that under the limiting condition of  $L \rightarrow \infty$  (i.e. long channel device), Eq.(35) results in

$$\psi_{s \min L} = \lim_{L \rightarrow \infty} \psi_{s \min} = V_G - V_{fb} - \lambda^2 \frac{qN_p}{2\epsilon_{si}} \exp(-B^2) \quad (39)$$

since  $k_1 \rightarrow 0$  and  $k_2 \rightarrow 0$  as  $L \rightarrow \infty$ .

Substituting  $\psi_{s \min L}$  by  $\psi_{s \min-th}$  from Eq.(37) in Eq.(39) and solving for  $V_G = V_{thL}$ , we may obtain

$$V_{thL} = \psi_{s \min-th} + V_{fb} + \frac{\lambda^2 qN_p}{2\epsilon_{si}} \exp(-B^2) \quad (40)$$

where  $V_{thL}$  represents the threshold voltage of the long-channel DG MOSFET device.

Using Eq.(40) in (37), we can express the threshold voltage  $V_{th}$  in terms of the  $V_{thL}$  as

$$V_{th}^2(1-4QR) + 2(2RD + 2QE - V_{thL})V_{th} + (V_{thL}^2 - 4DE) = 0 \quad (41)$$

which can be solved to express the threshold voltage of short-channel device as

$$V_{th} = -(2RD + 2QE - V_{thL})(1-4QR)^{-1} + \left( (2RD + 2QE - V_{thL})^2 - (1-4QR)(V_{thL}^2 - 4DE) \right)^{\frac{1}{2}} \times (1-4QR)^{-1} \quad (42)$$

It may be noted from (38) and (40) that  $V_{th}$  can also be expressed as

$$V_{th} = V_{thL} - \Delta V_{th} \quad (43)$$

where,

$$\Delta V_{th} = 2\sqrt{(D - QV_{th})(E - RV_{th})} \quad (44)$$

is the change in the threshold voltage due to short-channel effects, which is called the threshold voltage roll-off of the device.

Now, substituting  $V_{th} = V_{thL} - \Delta V_{th}$  from Eq.(43) in the right hand side of Eq.(44), we can obtain

$$\Delta V_{th}^2 \left( \frac{1}{4} - QR \right) + (2QRV_{thL} - DR - EQ)\Delta V_{th} + \left\{ (DR + EQ)V_{thL} - QRV_{thL}^2 - DE \right\} = 0 \quad (45)$$

Clearly, the threshold roll-off  $\Delta V_{th}$  can be obtained by solving Eq.(45). However, it may be mentioned that for practical devices,  $\alpha = \frac{L}{\lambda} \gg 1$  which implies

$\exp(\alpha) \gg 1$ ,  $Q \approx \exp(-\alpha)$  and  $R \approx 1$ . Under the assumption that  $\exp(-\alpha) \ll \frac{1}{4}$  (which is observed to be valid for the present model), we can approximately express the threshold roll-off  $\Delta V_{th}$  as

$$\Delta V_{th} = 2(D+E'\exp(-\alpha) - 2\exp(-\alpha)V_{thL}) + 2\sqrt{(D+E'\exp(-\alpha) - 2\exp(-\alpha)V_{thL})^2 - C} \quad (46)$$

where,

$$C = V_{thL}(D+E'\exp(-\alpha)) - D'E' - \exp(-\alpha)V_{thL}^2 \quad (47)$$

$$D' = \left( V_{bi} + V_{fb} + \frac{\lambda^2 qN_p}{2\epsilon_{si}} \exp(-B^2) + V_{DS} \right) \exp(-\alpha) \quad (48)$$

$$E' = V_{bi} + V_{fb} + \frac{\lambda^2 qN_p}{2\epsilon_{si}} \exp(-B^2) + V_{DS} \exp(-\alpha) \quad (49)$$

Note that  $\Delta V_{th} \rightarrow 0$  as  $L \rightarrow \infty$  (i.e.  $\alpha \rightarrow \infty$ ) which implies that  $V_{th} = V_{thL}$  for long-channel device. Thus, the threshold voltage of short-channel DG-MOSFETs can be obtained either from Eq.(41) or by using the values of  $V_{thL}$  and  $\Delta V_{th}$  in Eq.(42) from Eqs.(39) and (44) respectively.

### 3 Results and discussion

This section presents some theoretical and ATLAS™ simulation results of the minimum surface potential

( $\psi_{s\min}$ ) and threshold voltage ( $V_{th}$ ) of Gaussian doped DG MOSFETs. In Fig.2 the variation of the surface potential  $\psi_s$  along the channel length is plotted for the parameter values of  $L=65\text{nm}$ ,  $t_{si}=20\text{nm}$ ,  $t_{ox}=1.5\text{nm}$ ,  $V_{bi}=0.868\text{V}$ ,  $R_p=10\text{nm}$ ,  $\sigma_p=5\text{nm}$  and tungsten as a gate metal having work function  $\Phi_m=4.63\text{V}$  and various combination of gate-source  $V_G$ , and drain-source voltage  $V_{DS}$ .

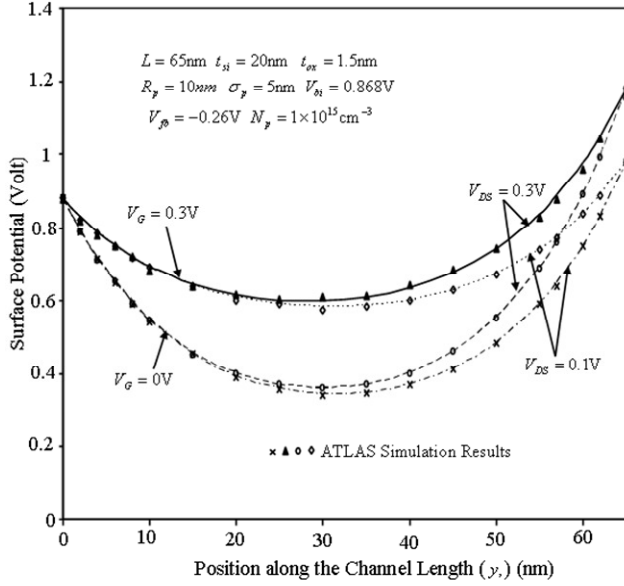


Fig.2: Variation of Si-SiO<sub>2</sub> interface potential (surface potential,  $\psi_s$ ) along the channel length for different value of gate

It is found that as the drain to source voltage  $V_{DS}$  is increased for a fixed value of  $V_G$ , the minimum surface potential is elevated, resulting in the significant decrease in the channel barrier. The minimum surface potential  $\psi_{s\min}$  shifts towards the source with the increase in the drain-source voltage  $V_{DS}$ . The magnitude of surface potential can also be elevated by applying higher gate-source voltage  $V_G$ . The results in Fig.2 show that the reduction in source-channel barrier, commonly known as drain induced barrier lowering (DIBL) in DG MOSFETs can occur due to the increase in the drain-source voltage as well as gate-source voltage. Figure 3 shows the long channel threshold voltage

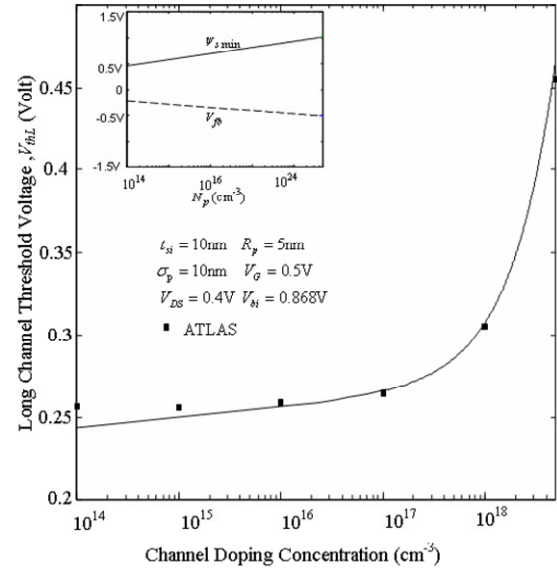


Fig.3. Long channel threshold voltage  $V_{thL}$  variation with the peak channel doping  $N_p$ . the long channel threshold voltage increases rapidly after channel doping value of  $10^{17}\text{cm}^{-3}$ .

$V_{thL}$  for different doping variation  $N_p$  for the device parameter values shown in the figure. It is observed that threshold voltage is increasing with a slow rate up to the peak channel doping of  $10^{17}\text{cm}^{-3}$  and rises suddenly above the said doping level. It is because of the cancellation of the doping sensitivities on  $V_{fb}$  and  $\psi_{s\min}$  from the sum of the first two components of Eq.(40) (see the inset in Fig.3) and relatively extremely low contribution by the third term of the said equation. While for the doping values higher than  $10^{17}\text{cm}^{-3}$ , the third term dominates and the  $V_{thL}$  rises sharply. Figure 4 shows the variation of threshold voltage with the channel length  $L$  for three different values of peak channel doping and  $t_{si}=10\text{nm}$ ,  $t_{ox}=1.5\text{nm}$  and  $\sigma_p=10\text{nm}$ . The position of peak doping is fixed at the centre of the silicon channel to maintain the symmetry of device. It is clear from the Fig.4 that threshold voltage is going down for the shorter channel length devices for the constant value of the doping which can be explained by the charge sharing concept in the channel region [17]. Threshold voltage is also increased for the higher value of peak channel

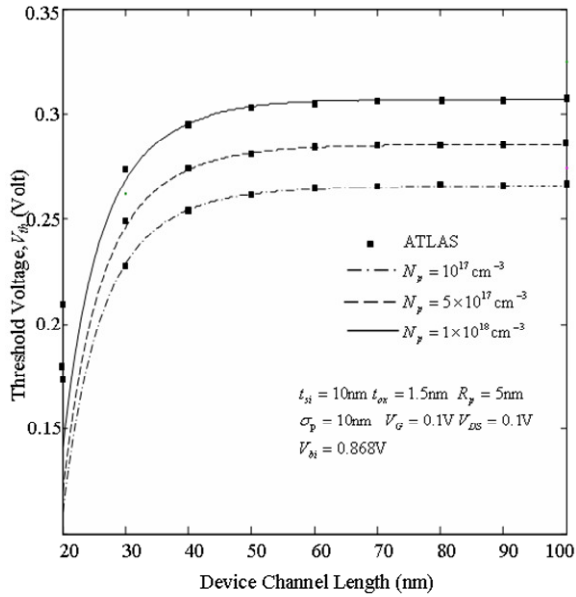


Fig.4: Demonstration of threshold voltage,  $V_{th}$  variation with the device channel lengths ( $L$ ) the three different values of the peak channel doping ( $N_p$ ).

The threshold voltage  $V_{th}$  degrades for the lower device channel length and elevate for higher doping. The symbols are the ATLAS device simulator results

doping  $N_p$ . Figure 5 shows the threshold voltage roll-off,  $\Delta V_{th}$  with the channel length for the three different values of the silicon channel thickness of 5nm, 8nm and 10nm. It is observed that the roll-off increases for the sub 60nm [11] channel length regime because of the dominant roles of short channel effects. It is also further noted that for lower values of silicon channel thicknesses  $t_{si}$ , the roll-off in threshold voltage is relatively low compared to the higher channel thicknesses. The shift in the threshold voltage  $\Delta V_{th}$  with lower channel length  $L$  for different oxide thickness is shown in the Fig.6. For higher gate oxide thickness, threshold voltage roll-off increases severely. All the presented results are well matched with the 2D ATLAS™ simulation results except for 20 nm channel length. It may be mentioned here that the quantum mechanical effects (QME) could play a significant role in determining the subthreshold characteristics of the DG MOS

devices with dimensions comparable with the de-Broglie

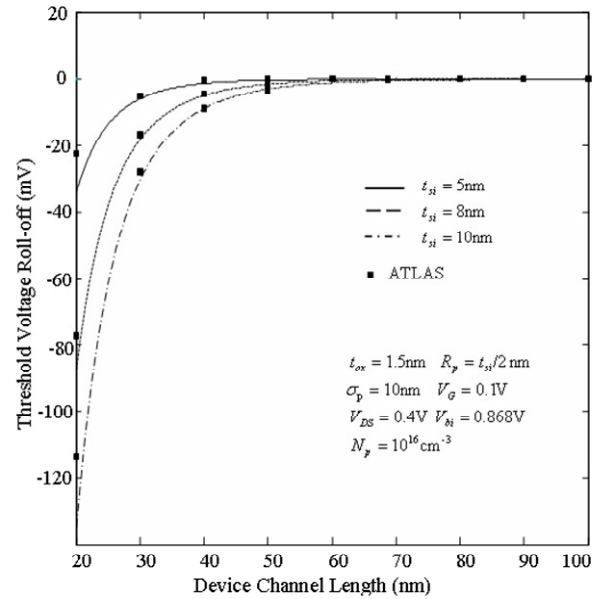


Fig.5: Variation of threshold voltage shift  $\Delta V_{th}$  with channel lengths for three different values of silicon channel thickness  $t_{si}$  of 5nm, 8nm and 10nm. Figure demonstrates that threshold voltage shift in DG MOSFET goes down for the thinner channel thickness

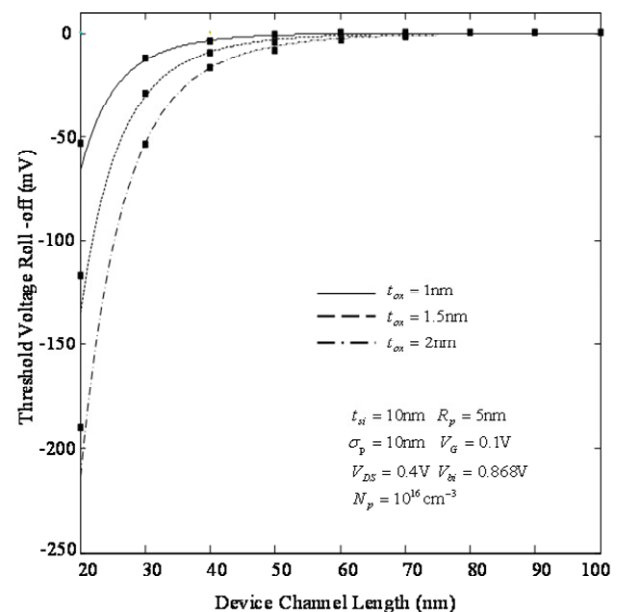


Fig.6: Depiction of threshold voltage roll-off  $\Delta V_{th}$  variation with the channel length for three different

values of oxide thickness. It is noted that threshold voltage roll off decreases severely for the higher oxide channel thickness. Symbols are ATLAS™ simulation results.

wavelength. The above discrepancy may be attributed to the QME which has been neglected for the simplicity of our presented model.

## 4 Conclusion

A two dimensional analytical model for the potential distribution and threshold voltage of symmetric DG MOSFETs with vertical Gaussian doping profile in the channel is proposed in this paper. The effects of doping profile parameters and device parameters on the threshold voltage of the short-channel and long-channel devices are discussed. The model results are found to be well matched with the commercially available 2D ATLAS™ device simulation results for channel lengths above 30nm. The present model could be useful for determining the subthreshold characteristics of a real DG MOSFET where a Gaussian like doping profile is expected to occur due to many implantation techniques being used during fabrication process.

### References:

- [1] A. Cerdeira, B. Iñiguez, and M. Estrada, "Compact model for short channel symmetric doped Double-Gate MOSFETs," *Solid-State Electron*, 52, 1064 (2008)
- [2] H. Lu, W.-Y. Lu, and Y. Taur, "Effect of body doping on Double-Gate MOSFET characteristics," *Semicond. Sci. Technol.*, 23, 015006 (2008)
- [3] M. Reyboz, O. Rozeau, T. Poiroux, P. Martin, and J. Jomaah, "An explicit analytical charge-based model of undoped independent Double-Gate MOSFET," *Solid-State Electron.*, 50, 1276(2006)
- [4] R. K. Sharma, R. Gupta, M. Gupta, and R. S. Gupta, "Graded channel architecture: the solution for misaligned DG FD SOI n-MOSFETs," *Semicond. Sci. Technol.*, 23, 075041(2008)
- [5] A. Cerdeira, O. Moldovan, B. Iñiguez, and M. Estrada, "Modeling of potentials and threshold Voltage for symmetric doped Double-Gate MOSFETs," *Solid-State Electron.*, 52,830 (2008)
- [6] D. Munteanu, J.-L. Autran, X. Loussier, S. Harrison, R. Cerutti, and T. Skotnicki, "Quantum short-channel compact modelling of drain-current in Double-Gate MOSFET," *Solid-State Electron.*, 50,680(2006).
- [7] J. L. Autran, D. Munteanu, M. Bescond, M. Houssa, and A. Said, "A simulation analysis of FIBL in decananometer Double-Gate MOSFETs with high-[kappa] gate dielectrics," *J. Non-Crystall. Solids*, 351, 1897 (2005).
- [8] J. W. Han, C. J. Kim, and Y. K. Choi, "Universal potential model in tied and separated Double-Gate MOSFETs with consideration of symmetric and separated asymmetric structure," *IEEE Trans. Electron Devices*, 55, 1472(2008)
- [9] S. Bhattacharjee and A. Biswas, "Modeling of threshold Voltage and subthreshold slope of nanoscale DG MOSFETs," *Semicond. Sci. Technol.*, 23, 015010 (2008)
- [10] A. Tsormpatzoglou, C.A. Dimitriadis, R. Clerc, G. Pananakakis and G.Ghibaud, "Threshold Voltage model for short-channel undoped symmetrical Double Gate MOSFETs," *IEEE Trans. Electron Devices*, 55, 2512 (2008)
- [11] H. A. El Hamid, J. R. Guitart, and B. Iniguez, "Two-dimensional analytical threshold voltage and subthreshold swing models of undoped symmetric Double-Gate MOSFETs," *IEEE Trans. Electron Devices*, 54, 1402 (2007)
- [12] H. Kang, J.W. Han and Y.K.Choi, "Analytical threshold voltage model for Double-Gate MOSFETs with localized charges," *IEEE Electron Device Lett.*, 29, 927 (2008)
- [13] A. Kranti and G.A. Armstrong, "Engineering source/drain extension regions in nano scale double gate SOI MOSFETs: Analytical model and design considerations," *Solid-State Electron*, 50, 437 (2006)
- [14] G. Zhang Z. Shao and K Zhou, "Threshold voltage model for short channel FD-SOI MOSFETs with vertical Gaussian profile," *IEEE Trans. Electron Devices*, 55, 803(2008)
- [15] S. Chen and J. B. Kuo, "Deep Submicrometer Double-Gate Fully-Depleted SOI MOS Devices: A Concise Short-Channel Effect Threshold Voltage Model Using a Quasi-2D Approach" *IEEE Trans. Electron Devices*, 43, 1387 (1996)



[16] Silvaco Int. 2004: ATLAS User's Manual A 2D numerical device simulator  
<http://www.silvaco.com>.

[17] S. Cristoloveanu, "Silicon on insulator technologies and devices: from present to future" Solid-State Electron, 45,1403 (2001)